Improved Climatological Characterization of Optical Turbulence for Space Optical Imaging and Communications

Randall J. Alliss and Billy D. Felton

Northrop Grumman Information Systems
3975 Virginia Mallory Drive
Chantilly, VA 20151

Abstract

Optical turbulence (OT) acts to distort light in the atmosphere, degrading imagery from astronomical or other telescopes. In addition, the quality of service of a free space optical communications link may also be impacted. Some of the degradation due to turbulence can be corrected by adaptive optics. However, the severity of optical turbulence, and thus the amount of correction required, is largely dependent upon the turbulence at the location of interest. Therefore, it is vital to understand the climatology of optical turbulence at such locations. In many cases, it is impractical and expensive to setup instrumentation to characterize the climatology of OT, particularly for OCONUS locations, so simulations become a less expensive and convenient alternative.

The strength of OT is characterized by the refractive index structure function Cn^2, which in turn is used to calculate atmospheric seeing parameters. While attempts have been made to characterize Cn^2 using empirical models, Cn^2 can be calculated more directly from Numerical Weather Prediction (NWP) simulations using pressure, temperature, thermal stability, vertical wind shear, turbulent Prandtl number, and turbulence kinetic energy (TKE). In this work we use the Weather Research and Forecast (WRF) NWP model to generate Cn^2 climatologies in the planetary boundary layer and free atmosphere, allowing for both point-to-point and ground-to-space seeing estimates of the Fried Coherence length (r_o) and other seeing parameters. Simulations are performed using the Maui High Performance Computing Centers (MHPCC) Mana cluster.

The WRF model is configured to run at 1km horizontal resolution over a domain covering several hundreds of kilometers. The vertical resolution varies from 25 meters in the boundary layer to 500 meters in the stratosphere. The model top is 20 km. We are interested in the variations in Cn^2 and the Fried Coherence Length (r_o). Nearly two years of simulations have been performed over various regions including the Desert Southwest and Haleakala and Mauna Kea on Hawaii. A recent improvement to our modeling over Hawaii was performed by using a more representative land usage dataset. Simulations indicate that the vast lava fields which characterize the Big Island to the shoreline have a large impact on turbulence generation. The same turbulence characteristics are also present in the simulations on the Southeastern face of Haleakala. Turbulence is greatest during the daytime when the lava fields produce tremendous heat fluxes. Good agreement is found when the WRF simulations are compared to *in situ* data taken from the Thirty Meter Telescope (TMT) on Mauna Kea. The TMT study used a variety of seeing instruments which provided data day and night. Both the WRF simulations and TMT showed r_o values bottoming out in the 3-4 cm range during daytime at Mauna Kea. Simulations are also performed over White Sands New Mexico and will be reported on at the conference. Results of these analyses are assisting engineers in developing state of the art adaptive optics designs. Detailed results of this study will be presented at the conference.

1. Introduction

With High Performance Computing (HPC) platforms becoming much more affordable and accessible, simulations of physical parameters in the atmosphere are easily performed. An excellent example of this is free space optical turbulence (OT). OT is an important atmospheric phenomenon, particularly for astronomers, because of the impact it has on seeing. Small-scale temperature and moisture fluctuations in the atmosphere result in fluctuations of the refractive index. The wave front of radiation traveling through the atmosphere changes as it encounters inhomogeneities in the refractive index, degrading optical image quality. The intensity of the turbulent fluctuations of the atmospheric refractive index is described by the refractive index structure function, C_n^2. The ability to quantify the amount of OT above an observatory and to understand its vertical distribution is vital and can impact decisions on adaptive optics design, observatory scheduling, and site selection for new observatories. Although instruments have been developed to characterize OT, they are expensive to maintain over long durations of time and the quality is limited.

Numerical simulations of OT are an attractive alternative to local observations in regions where infrastructure (i.e., electrical power) is lacking. Numerical simulations offer many advantages over direct measurements. These advantages include a three-dimensional description of C_n^2 over regions of interest, simulations that can be performed anywhere on earth at any time, and the ability to provide forecasts of OT that could be used for observational scheduling purposes. The reliability of these types of simulations for describing the climatology of OT has recently been shown to be quite good.

Our approach to simulate OT employs a model used to predict tropospheric weather. These models are referred to by the meteorological community as Numerical Weather Prediction (NWP). NWP models are routinely used by meteorologists to predict everyday weather. However, in this application the model is modified to make simulations of C_n^2. In this paper we describe how NWP is leveraged to simulate OT and present various results along with intercomparisons to direct observations of integrated OT.

2. Technical Approach

In this study we use version 3.0 of the Weather Research and Forecasting (WRF) model developed jointly by the National Center for Atmospheric Research (NCAR) and the National Oceanic and Atmospheric Administration (NOAA) (Skamarock et al., 2008). WRF is a mesoscale NWP model developed for the prediction of weather and is routinely used by the National Weather Service and other forecasting services. The model is based on the Navier Stokes equations, which are solved numerically on a three-dimensional grid. Four basic atmospheric properties are simulated by the model from which all others variables are derived. These properties are wind, pressure, temperature, and atmospheric water vapor.

This study used the WRF model to develop climatology of OT over the Hawaiian Islands including the summits on Maui and the Big Island. In addition, it performed simulations over the desert South West and in New Mexico. The following sections describe the model setup, modifications to the code, and derivation of OT parameters followed by results of simulations to date.

a. Model Setup

WRF is used to simulate daily meteorological conditions for Hawaii, Southern California and New Mexico for the 2008-2009 time periods. The model is configured at 1-km horizontal resolution with dimensions of 273x273 grid points and 83 vertical levels. The resolution of the vertical levels is approximately 50-m resolution below 2 km above ground level (AGL), 125 m for 2–12 km AGL, and 500 m up to the model top (50 millibars). Simulations are initialized at 1200 UTC directly from the 36-km Global Forecasting System (GFS) analysis produced by the National Weather Service. Lateral boundary conditions are provided out to 27 hours by three-hourly GFS forecasts. This allows for filtering out model "spin-up" by excluding the first three simulation hours, while still capturing the full 24-hour diurnal cycle. Selected physics and diffusion options are summarized in Table 1.The model was reinitialized each day during the two year period.

Table 1. Physics and diffusion settings used in WRF model for this study

Time Integration	RK3
Time Step	2 sec
Horizontal/Vertical Advection	Fifth/Third order
Explicit Diffusion	Physical space 2D deformation, no sixth order
Boundary Layer Physics	Mellor, Yamada, Janjic (MYJ)
Surface Layer	Janjic Eta
Land Surface	Noah
Shortwave/Longwave Radiation	Dudhia/RRTM
Microphysics	WSM6
Cumulus Parameterization	None

b. Model Modifications

The minimum turbulence kinetic energy (TKE) permitted in the Mellor-Yamada-Janjic (MYJ) scheme had to be modified. The default setting gives TKE values >0.1 m^2s^{-2}, resulting in unrealistically large values of C_n^2 in the free atmosphere. Following Gerrity et al. (1994), the minimum TKE limit was changed to 10^{-5} m^2s^{-2}. The second modification involves the eddy diffusivities of heat and momentum (K_H and K_M, respectively). In the original MYJ scheme, these variables are given by

$$K_h = l_q S_H \quad , K_h = l_q S_M,$$

Where l is the mixing length, $q = \sqrt{2TKE},$ and $S_H,$ and $S_M,$ are functions of TKE, mixing length, buoyancy, and vertical wind shear (Mellor and Yamada, 1982). In the modified version these relationships are unchanged for neutral and unstable conditions. However, when the gradient Richardson number (Ri) > 0.01, an implementation by Walters and Miller (1999) is followed whereby K_M is adjusted according to:

$$\frac{K_H}{K_M} = \begin{cases} \dfrac{1}{7Ri}, & for\ Ri \geq 1, \\ \dfrac{1}{6.873Ri + \dfrac{1}{1+6.873Ri}}, & for\ 0.01 < Ri \leq 1. \end{cases}$$

The $\frac{K_H}{K_M}$ equation was first proposed by Kondo et al. (1978). The Kondo equation decreases $\frac{K_H}{K_M}$ with increasing Ri, effectively increasing the TKE production by vertical wind shear. This is necessary to generate free atmospheric turbulence that is commonly associated with jet streams. Without this change the model rarely produces TKE larger than the model's minimum value, something that is considered unrealistic when compared to many global thermosonde measurements (Ruggiero, personal communication, 2008).

Recent improvements to the land usage modeling have been made for the Hawaiian domain. In the original research we used a very simple land usage dataset which was not very representative of the actual land usage. This dataset over estimated the amount of lava rock particularly for the island of Maui. The result of this over estimate yielded surface heat fluxes which were too strong and thus over estimated the severity of turbulence. Figure 1

shows the original land usage data set and the recent replacement. Note in Figure 1b the much more detailed land usage information. This has a measurable impact on the quality and accuracy of the optical turbulence simulations.

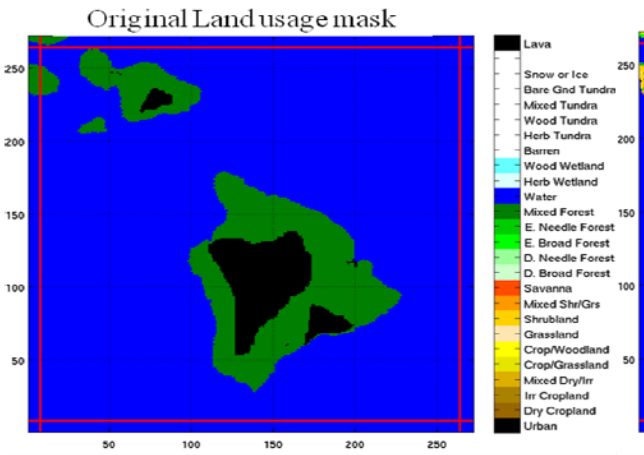

Figure 1a. Improved land usage data.

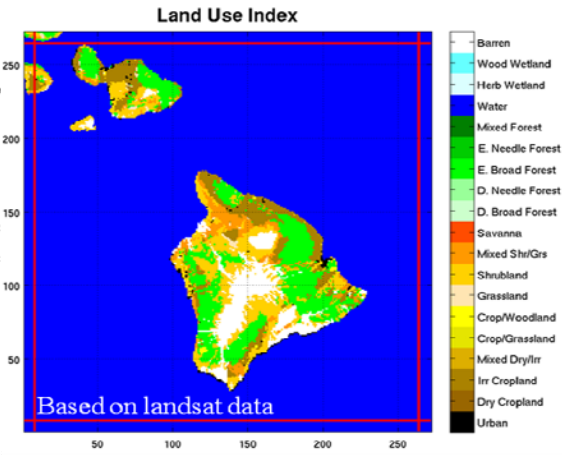

Figure 1b. Original land usage data.

c. Derivation of Seeing

This study is interested in the vertical distribution of the refractive index structure function C_n^2. When turbulence is locally homogeneous and isotropic, C_n^2 is related to changes in the refractive index. Large values of C_n^2 correspond to increasing changes in the refractive index and thus greater turbulence. Tatarskii (1971) derived an alternative expression for the structure function parameter applicable for optical wavelengths:

$$C_n^2 = \left(\frac{79 * 10^{-8} P}{T^2} \right)^2 C_T^2$$

where P is atmospheric pressure, T is air temperature, and C_T^2 is the structure function parameter for temperature. C_T^2 is given by:

$$C_T^2 = a^2 \left(\frac{K_H}{K_M} \right) L_o^{\frac{4}{3}} \left(\frac{\partial \theta}{\partial Z} \right)^2$$

Where a^2 is an empirical constant, L_o is the outer length scale of turbulence (i.e., the upper bound of the inertial subrange), and $\left(\frac{\partial \theta}{\partial Z} \right)$ is the vertical gradient of potential temperature. Following Walters and Miller (1999), a^2 is set to 2.8 and calculation of the outer length scale of turbulence in the thermally stable conditions is approximated from Deardorff (1980):

$$L_o = 0.76 \sqrt{\frac{TKE}{N}}$$

where *N* is the Brunt-Vaisala frequency. In thermally unstable conditions, L_o is related to the depth of the unstable boundary layer.

In this study we also compute Fried's Coherence Length (r_o), which is a measure of phase distortion of an optical wave front by turbulence. r_o can vary rapidly over time and from one point of the sky to another. This parameter represents the integrated effect of turbulence along a line of sight. Larger (smaller) values of r_o are indicative of less (more) turbulence and better seeing. After Fried (1965), it is calculated by integrating C_n^2 along a path, *z*:

$$r_o = \left[0.423 \left(\frac{2\Pi}{\lambda} \right)^2 \int_0^\infty C_n^2(z) dz \right]^{-3/5}$$

3. Results

Three-dimensional turbulence simulations were made over the state of Hawaii (Figure 2) once per day during the two year period. The figure indicates the terrain heights in meters above sea level. Not the three main peaks on the islands including Haleakala on Maui, and Mauna Loa and Mauna Kea on the Big Island. These islands are characterized by steeply rising volcanic mountains, ridges and ravines. The windward sides of the islands are subject to the Northeast trade winds which blow the majority of the year. These trades produce wet conditions on the windward side of the islands compared to the leeward side. Clouds are typical trapped below the trade wind boundary layer around 2km making the summits quite clear.

The WRF simulations were generated at the Maui High Performance Computing Center (MHPCC) and took approximately 2400 wall clock hours to complete.

Because the model output contains many terabytes of information a tool was developed to facilitate analysis of these data. This tool makes use of the Python scripting language to control data ingest and graphical user interface attributes and Matlab for data display. The tool provides a two-dimensional view of the topography over the selected domain. The tool allows the user to load any month or year of data and to quickly look at two-dimensional plots of various seeing parameters including r_o, Θ_o and the Greenwood Frequency, f_G, as a function of time of day. This allows for analysis of how the turbulence may be distributed horizontally across the domain. The user may also look at the distribution of any of these parameters for a single vertical column in the domain.

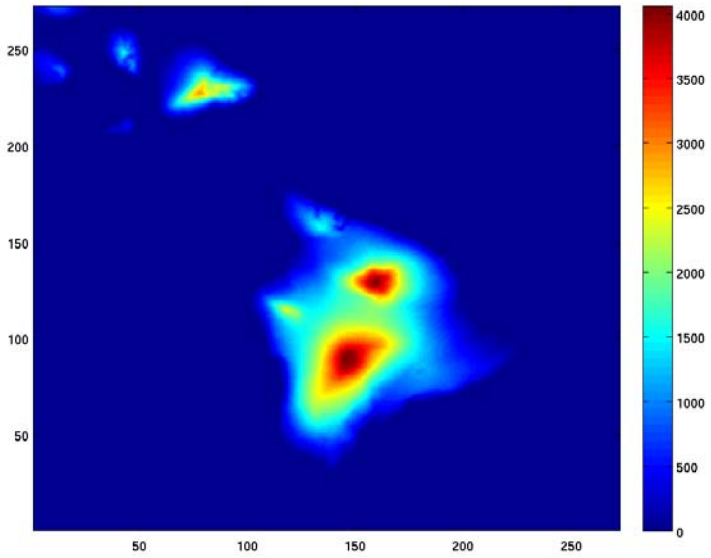

Figure 2. WRF Domain over the Hawaiian Islands. Terrain heights are in meters above sea level.

The mean r_o as a function of time of day is shown for the island of Maui in Figure 3a-d. The values are referenced to zenith and are valid at 500nm. The simulations indicate that the best seeing occurs just below the summit of Haleakala (9-11cm) with a relative minimum in r_o at summit level (7-9cm). At first glance this may not appear reasonable. However, simulations indicate surface winds are stronger at peak level compared to elevations only 200 meters below the peaks. There appears to be a minimum in wind speed immediately to the leeward side of the peaks, particularly at Haleakala. The majority of the turbulence developed by the model is in the surface layer so this is not unreasonable. Bradley et. al 2006 reports that with the prevailing

winds from the east to northeast, the air must cross over the caldera before reaching the observatories on Haleakala. This has the effect of increasing the turbulence immediately above the site. Since the WRF model was configured to have limited vertical resolution near the surface the model may be picking up on this process and over predicting the turbulence at summit level. It is also postulated that the better seeing produced in the WRF simulations below summit level are an effect of mountain blocking. We are in the process of trying to find surface observations below peak which will corroborate these findings. Figure 3 also indicates how the turbulence strength varies by time of day. Turbulence at 0400 (night) is at its weakest but this begins to reverse by 0800 when the sun is rising. During the middle of the day 1300 HST the turbulence strength is at its greatest. This is primarily due to the strong land heating by the sun. The trend reverses again as sunset is approached, 2000 HST. It is remarkable that the best seeing conditions are found in the west side of Haleakala where a shadowing effect is apparently at play.

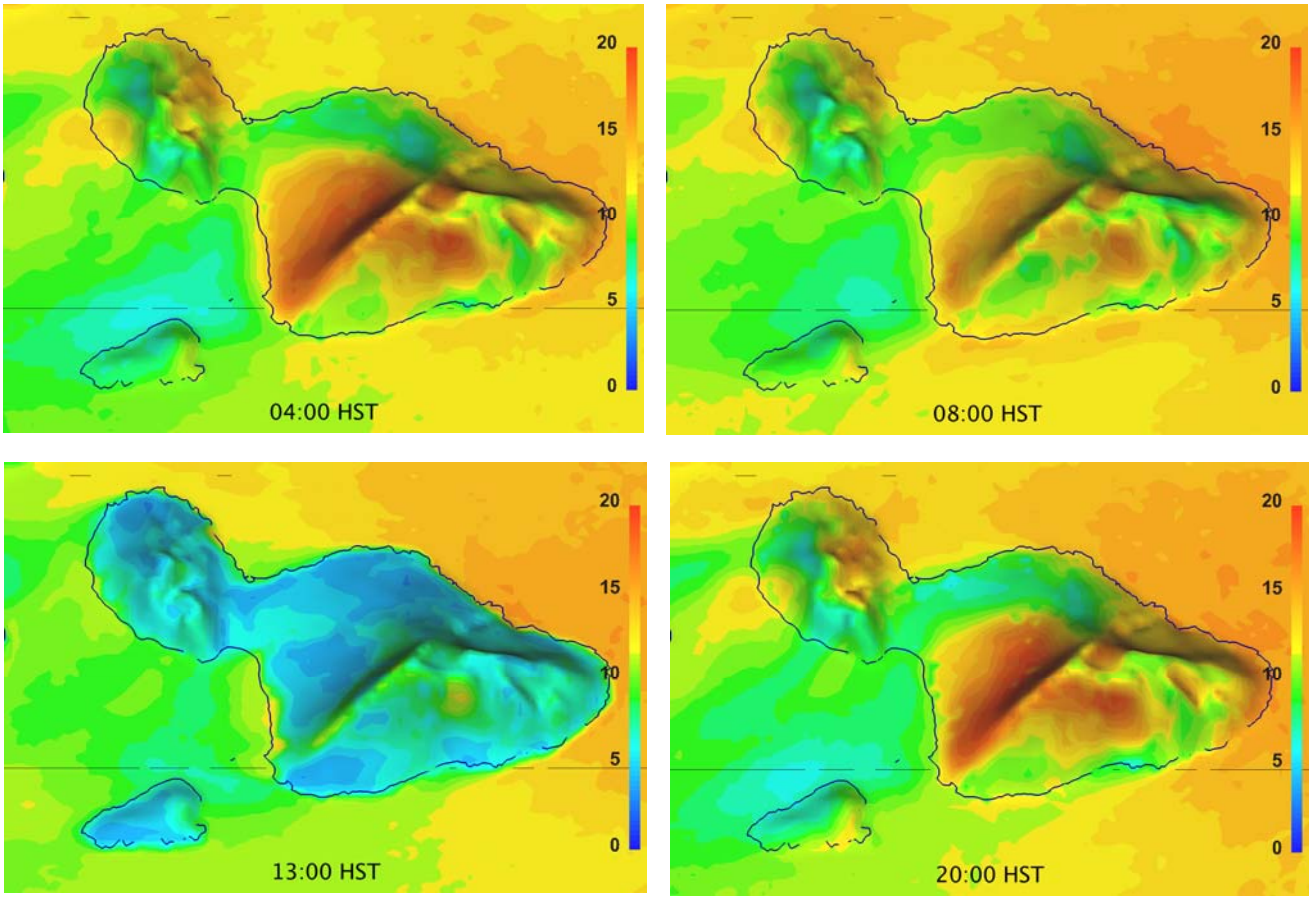

Figure 3. Mean r0 over island of Maui for a) Nighttime (upper left), b) sunrise (upper right), c) mid-afternoon (lower left) and d) sunset (lower right).
Data is referenced to zenith and is valid at 500 nm.

Figure 4 shows the impact of the improved land usage on the statistics of turbulence at Haleakala. The data is broken down by day and night. Figure 4a shows the cumulative distribution (CDF) of r_o at Haleakala with the original land usage data set (blue) and the new land usage data (red). Results indicate that turbulence is less severe than originally simulated. The 50% percentile r_o originally was 13 cm however this increases to approximately 15 cm with the improved land usage (Figure 4b). During daytime the 50% percentile r_o is approximately 9 cm with the original land usage data and nearly 12 cm with the improved land usage. The higher resolution and more accurate land usage data cuts down on the turbulence primarily because the summit is characterized by barren land as

opposed to lava. The heat capacity of barren soil is much larger than that of lava and therefore, this cuts down on the surface heat fluxes whether its day or night.

Figure 5 shows the impact of the improved land usage on simulations of optical turbulence at Mauna Kea. With respect to the original simulations shown in blue the new land usage (red) cuts down on the production of optical turbulence. The 50th percentile r_o is nearly 50% larger with the high resolution land usage day or not. Comparisons to the r_o data collected at the Thirty Meter Telescope on Mauna Kea with the WRF simulations agree very well. The distributions of r_o are within 1-2 cm.

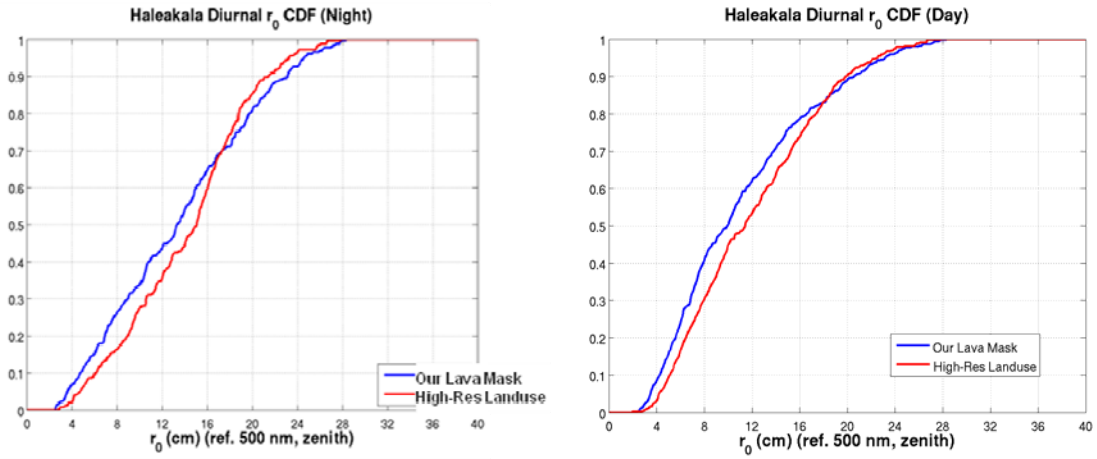

Figure 4. CDF of r_o for the summit of Haleakala at night (left) and during the daytime (right). More benign turbulence is found at the summit using the higher resolution land usage data.

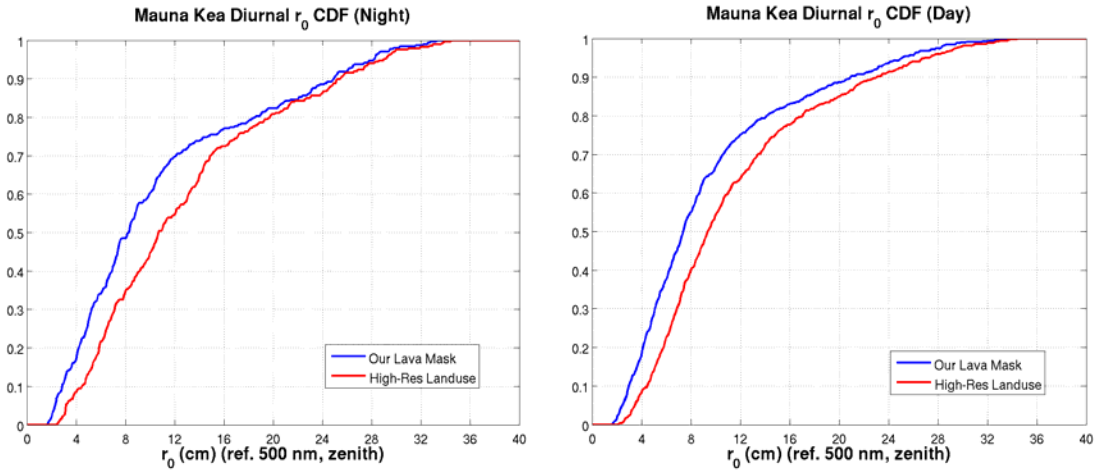

Figure 5. CDF of r_o for the summit of Mauna Kea at night (left) and during the daytime (right). More benign turbulence (~50%) is found at the summit using the higher resolution land usage data.

As indicated earlier, optical turbulence data is being used by optical communication engineers to estimate impact on performance. The NASA Lunar Atmosphere and Dust Environment Explorer (LADEE) will fly a lasercom terminal and conduct optical communications from an orbit around the moon back to earth. In selecting a ground site to receive the optical signal it's imperative to maximize the amount of cloud freeness. In order to do this, statistics of cloud freeness are developed from our GOES derived cloud retrieval software and converted into Cloud

Free Line of Sight (CFLOS) (Alliss et al. 2000, Alliss et.al 2004). An example is shown in Figure 6 to the right. The Monthly CFLOS at the summit of Haleakala between 1997 and 2009 are indicated. The mean CFLOS over the thirteen year period is approximately 70%, however, substantial variation by year is noted. A pathological month, in terms of CFLOS, was observed during March 2006. During this month the normally very clear summit was obscured by clouds nearly 80% of the time. This was corroborated by astronomers at the University of Hawaii. CFLOS conditions at other sites (not shown in this paper) in the desert South West also have high CFLOS comparable to the summit of Haleakala.

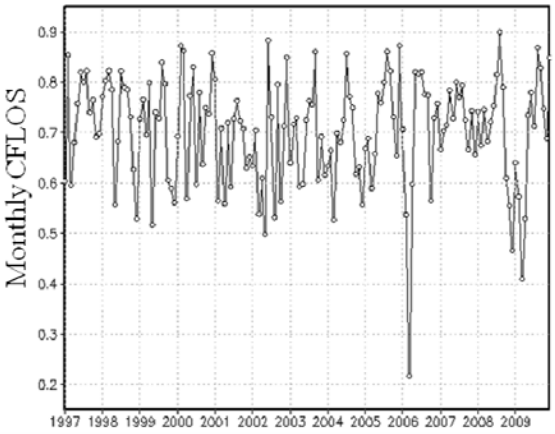

Figure 6. Monthly Cloud Free Line of Sight (CFLOS) for the summit of Haleakala, Maui

The turbulence is another factor which may influence site selection for an optical down link. Figure 7 below shows the diurnal variation of optical turbulence (r_o) at four locations including Haleakala, Dryden, CA, Table Mountain, CA and White Sands, NM. Results indicate that Haleakala has the most benign turbulence on the mean compare with the other three sites. They are nearly twice as large at Haleakala compared with the other sites. Note these values of r_o are referenced at 1550 nanometers and zenith which is the carrier wavelength of the signal. All sites show the classic diurnal variation with large r_o at night, followed by a steady decrease during the daylight hours and then a neutral event just before sunset.

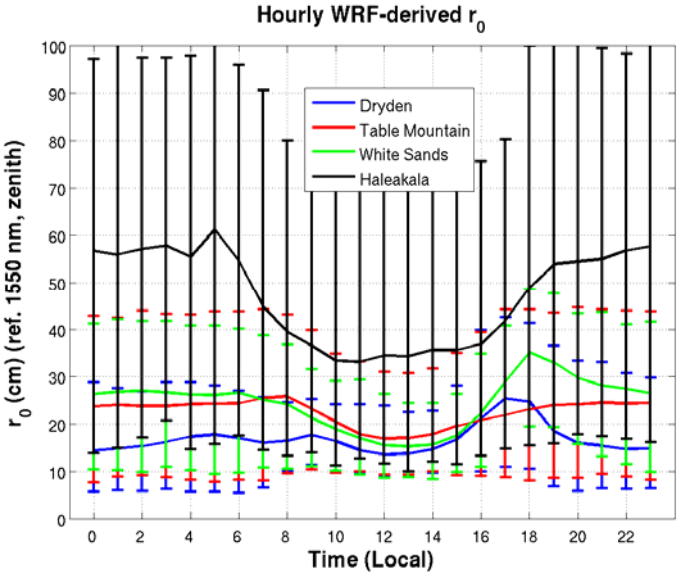

Figure 7. The diurnal variation in at four locations. The mean and 5th and 95th percentile of the data distribution are shown. Values are referenced to 1550 nm and zenith. Haleakala by far has the best seeing conditions.

In order to conduct a validation exercise we wanted to compare the WRF simulations of r_o with *in situ* data collected over an extended time frame. Data was obtained from the Advanced Technology Solar Telescope (ATST) Site Survey Working Group at the Mees Solar Observatory on Haleakala. ATST will be the largest solar telescope in the world, with unprecedented abilities to view details of the Sun *(ATST Site Survey Working Group Final Report, 2004)*. Using adaptive optics technology, ATST will be able to provide the sharpest views ever taken of the solar surface, which will allow scientists to learn even more about the Sun and solar-terrestrial interactions. The ATST seeing data was collected with a seeing monitor made up of two components: a Solar Differential Image Motion Monitor (S-DIMM) and an array of six scintillometers known as the Shadow Band Ranger (SHABAR). The S-DIMM measures the total value of r_o integrated from the observing height to the top of the atmosphere. The

SHABAR measures the steady and fluctuating intensity of sunlight in six detectors. It is used to estimate *Cn2(h)* and hence r_o as a function of height above the 8-m height at which the seeing monitor entrance aperture is mounted. The ATST seeing data obtained includes the time stamp of the measurement, the solar zenith angle, r_o at 8 and 28 meters, respectively and the surface winds and temperature. The ATST seeing data is collected during the daytime only and is valid between solar zenith angles of 5˚ and 85˚. Comparisons to the WRF simulations using the ATST data are therefore restricted to daytime. Figure 8 shows a comparison between WRF seeing and those obtained from the ATST dataset. Since the ATST data is referenced to the solar elevation angle of the sun the WRF data is referenced the same way to facilitate comparisons. Overall the WRF simulations agree best with the 8 meter ATST measurements, although WRF tends to underestimate the smallest values as well as the very largest. The WRF simulations agree very closely with the 28 meter estimates up to 4 cm but underestimate the larger values of r_o. We are unsure of the quality of the ATST measurements at very low sun angles. At these times the ATST data produces the largest r_o. Overall we believe the comparisons to be reasonable.

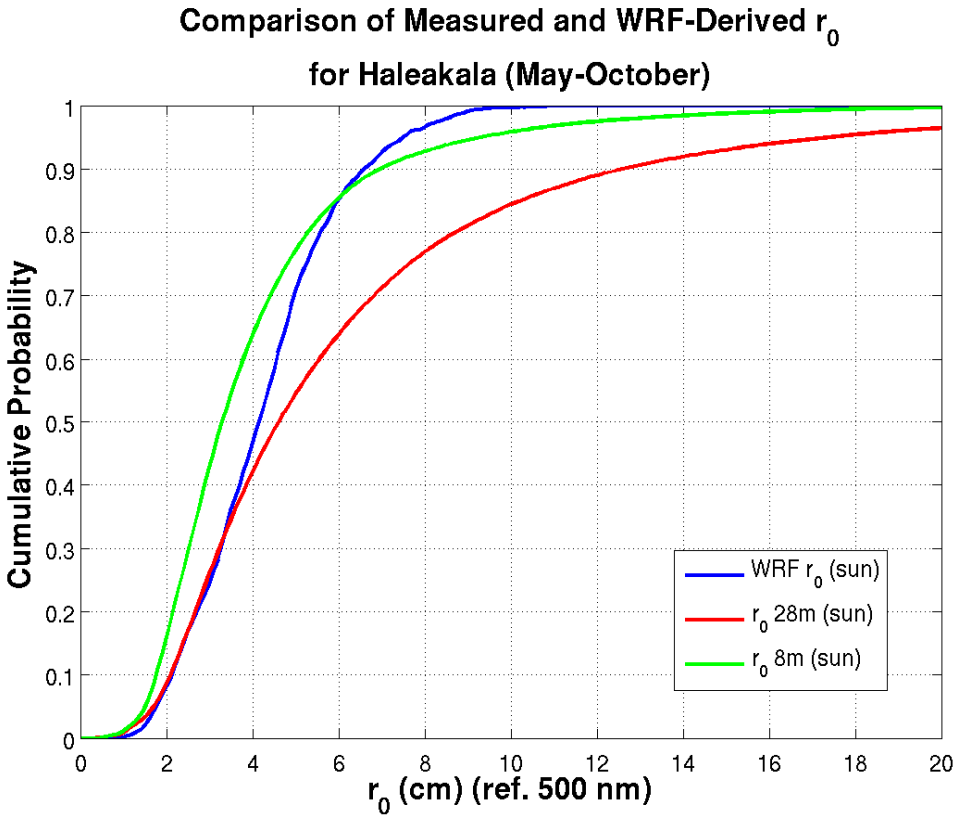

Figure 8. The cumulative distribution function (CDF) of r_o between WRF and ATST data. Data is referenced to zenith and is valid at 500 nm.

4. Summary and Conclusions

Simulations of OT were performed using the WRF model over the Hawaiian Islands and the desert South West. Although the WRF model is incapable of simulating the very smallest values of r_o, it is capable of generally describing the climatology of the region of interest. This makes the model very convenient to use over areas where observations are not possible. The model does an excellent job simulating the diurnal variation found in turbulence. Comparisons to the ATST data showed similar distributions. These simulations of optical turbulence are being used by designers of optical communication systems and for overall system risk reduction studies.

5. Acknowledgments

The authors thank the Maui High Performance Computing Center (*Mana*) and the Northrop Grumman IS HPC (*Argo*) center for providing simulation time on their clusters.

References

Alliss, R.J., R. L. Link, M. E. Craddock, "Mitigating the impact of clouds on optical communications," in *13th Conference on Satellite Meteorology and Oceanography*, American Meteorological Soc., September 2004.

Alliss, R.J., M. E. Loftus, D. Apling, and J. Lefever, "The development of cloud retrieval algorithms applied to goes digital data," in *10th Conference on Satellite Meteorology and Oceanography*, pp. 330–333, American Meteorological Soc., January 2000.

ATST Site Survey Working Group Final Report, 2004: http://atst.nso.edu/files/docs/RPT-0021.pdf

Bradley, E.S., L.C. Roberts, L. W. Bradford, M. Skinner, D.A. Nahrstedt, M.F. Waterson and J.R. Kuhn, 2006: Characterization of Meteorological and Seeing Conditions at Haleakala. *Publications of the Astronomical Soc. of the Pacific*, **118:**172-182.

Deardorff, J. W., 1980: Stratocumulus-capped mixed layers derived from a three-dimensional model. *Bound.-Layer Meteor.*, **18**, 495–527.

Fried, D. L., 1965: Statistics of a geometric representation of wavefront distortion. *J. Opt. Soc. Amer.*, **55**, 1427–1435.

Gerrity, J. P., T. L. Black, and R. E. Treadon, 1994: The numerical solution of the Mellor-Yamada level 2.5 turbulent kinetic energy equation in the Eta model. *Mon. Wea. Rev.*, **122**, 1640–1646.

Kondo, J., O. Kanechika, and N. Yasuda, 1978: Heat and momentum transfers under strong stability in the atmospheric surface layer. *J. Atmos. Sci.*, **35**, 1012–1021.

Mellor, G. L., and T. Yamada, 1982: Development of a turbulence closure model for geophysical fluid problems. *Rev. Geophys. Space Phys.*, **20**, 851–875.

Skamarock, W. C., J. B. Klemp, J. Dudhia, D. O. Gill, D. M. Barker, M. G. Duda, X.-Y. Huang, W. Wang, and J. G. Powers, 2008: A description of the advanced research WRF version 3. NCAR Technical Note, NCAR/TN-475+STR, 113 pp.

Tatarskii, V. I., 1971: The effects of the turbulent atmosphere on wave propagation. Technical Report, U.S. Department of Commerce, NTIS TT-68-50464, 472 pp.

Walters, D. L., and D. K. Miller, 1999: Evolution of an upper-tropospheric turbulence event—comparison of observations to numerical simulations. *Preprints, 13th Symposium on Boundary Layer Turbulence*, AMS, 157–160, Dallas, TX.